Cd^{2+} Regulation of the Hyperpolarization-activated Current I_{AB} in Crayfish Muscle

ALFONSO ARAQUE, DANIEL CATTAERT,* and WASHINGTON BUÑO

From the Instituto Cajal, CSIC, E-28002 Madrid, Spain; and *Laboratoire de Neurobiologie et Mouvements, CNRS, F-13402 Marseille, France

ABSTRACT The effects of Cd^{2+} on the hyperpolarization-activated K^+-mediated current called I_{AB} (Araque, A., and W. Buño. 1994. *Journal of Neuroscience.* 14:399–408.) were studied under two-electrode voltage-clamp in opener muscle fibers of the crayfish *Procambarus clarkii*. I_{AB} was reversibly reduced by extracellular Cd^{2+} in a concentration-dependent manner, obeying the Hill equation with IC_{50} = 0.452 ± 0.045 mM and a Hill coefficient of 1 (determined from the maximal chord conductance of I_{AB}). Cd^{2+} decreased the I_{AB} conductance (G_{AB}) and shifted its voltage dependence towards hyperpolarized potentials in a similar degree, without affecting the slope of the voltage dependence. The I_{AB} activation time constant increased, whereas the I_{AB} deactivation time constant was not modified by Cd^{2+}. The I_{AB} equilibrium potential (E_{AB}) was unmodified by Cd^{2+}, indicating that the selective permeability of I_{AB} channels was not altered. I_{AB} was unaffected by intracellular Cd^{2+}. The Cd^{2+}-regulation of I_{AB} did not depend on $[K^+]_o$, and the effects of $[K^+]_o$ on I_{AB} were unchanged by Cd^{2+}, indicating that Cd^{2+} did not compete with K^+. Therefore, Cd^{2+} probably bound to a different site to that involved in the K^+ permeability pathway. We conclude that Cd^{2+} affected the gating of I_{AB} channels, interfering with their opening but not with their closing mechanism. The results can be explained by a kinetic model in which the binding of Cd^{2+} to the I_{AB} channels would stabilize the gating apparatus at its resting position, increasing the energy barrier for the transition from the closed to the open channel states.

INTRODUCTION

The investigation of the block and regulation of membrane currents by different substances has provided useful insights into the structure and function of voltage-gated ionic channels (see e.g., Armstrong, 1975; Hille, 1992). For example, the analysis of channel block has supplied fundamental knowledge on the mechanisms of ion permeation and specificity, gating, activation, deactivation, and inactivation, and on the structure of numerous types of voltage-gated channels (e.g., Woodhull, 1973; Armstrong, 1975; Gay and Stanfield, 1977; Standen and Stanfield, 1978; Catterall,

Address correspondence to Dr. Washington Buño, Instituto Cajal, Avenida Doctor Arce 37, E-28002 Madrid, Spain.

J. GEN. PHYSIOL. © The Rockefeller University Press · 0022-1295/95/06/0725/20 $2.00
Volume 105 June 1995 725–744

1980; Nachsen, 1984; Lansman, Hess, and Tsien, 1986; Matsuda, Saigusa, and Irisawa, 1987; Swandulla and Armstrong, 1989; Lester, 1991; Mlinar and Enyeart, 1993).

Recently, a hyperpolarization-activated current termed I_{AB}, which underlies anomalous rectification in crayfish muscle, has been described (Araque and Buño, 1994). This time- and voltage-dependent current is selectively carried by K^+ and its activation curve is a function of the extracellular K^+ concentration ($[K^+]_o$). In addition, I_{AB} does not show instantaneous voltage-dependent activation, as occurs with the inward rectifier of vertebrate muscle and oocytes (Hagiwara and Takahashi, 1974; Sakmann and Trube, 1984; Matsuda et al., 1987). Moreover, whereas I_{AB} is unaffected by extracellular Ba^{2+}, Cs^+, or Rb^+, it is blocked by low extracellular concentrations of Cd^{2+} or Zn^{2+} (Araque and Buño, 1994).

The present study was aimed at characterizing the effects of Cd^{2+} on I_{AB} in an attempt to comprehend the mechanisms of its block and to supply information on the operation of the I_{AB} channels. The mechanisms of channel block have been described in terms of three general categories: (*a*) ionic pore occlusion; (*b*) modification of gating; and (*c*) shift in the voltage dependence (see Hille, 1992). In some cases, channel block has been exclusively associated to ionic pore occlusion, whereas modification of gating has been identified as regulation or modulation of channels. Because Cd^{2+} effects on I_{AB} could be explained by gating modification, we used the term regulation to refer to these effects.

We have found that the Cd^{2+} regulation of I_{AB} was dose dependent, and we provide evidence suggesting that Cd^{2+} modified the gating properties of I_{AB} channels, acting by binding to a site different to that involved in the K^+ permeability pathway. We propose a simple kinetic model that explains how the Cd^{2+} effects on the gating account for the shift in the voltage dependence of I_{AB} and the I_{AB} reduction. In that scheme, Cd^{2+} would stabilize the closed state of I_{AB} channels by increasing the energy barrier for the transition from the closed to the open channel states, whereas the energy barrier for the reverse transition from the open to the closed channel states was unmodified.

METHODS

Preparation

Opener muscles from the propodite of the first walking leg of crayfish (*Procambarus clarkii*) were isolated and transferred to a superfusion chamber (2 ml). Small crayfish (<5 cm) with short muscle fibers (<400 μm) were used for better space clamp characteristics.

Microelectrodes and Recordings

Fibers were impaled with two micropipettes filled with 1 M-KCl (1–5 MΩ). An Axoclamp-2A amplifier (Axon Instruments, Inc., Foster City, CA) was employed for two electrode voltage clamp recordings. Probe gains in the voltage clamp configuration were 1 and 10× for voltage and current electrodes, respectively. Voltage command pulses and injected currents were continuously monitored on a storage oscilloscope and stored on FM tape (0–1,250 Hz bandwidth; Hewlett-Packard, Model 3964a). The time required to reach the command pulse potential was ≤0.5 ms and there were no membrane potential (*Vm*) variations throughout the

pulse. Capacitive currents ended within ~5 ms. Recordings which did not meet these criteria were rejected. Pulse generation, data acquisition and analysis were done with a PC/AT personal computer (IBM) and pCLAMP software (Axon Instruments, Inc.) with a Lab Master TM-40 interface board (Scientific Solutions, Inc., Solon, OH).

Solutions

The control solution, modified from Van Harreveld (1936), was as follows (in millimolar): NaCl, 110; KCl, 5.4; $MgCl_2$, 16.1; Tetraethylammonium chloride, 100; Tris buffer 10; pH was adjusted to 7.2 with HCl. In this solution, depolarization-activated currents were eliminated or greatly reduced (Araque and Buño, 1994). In Cd^{2+} solutions, $CdCl_2$ was added in equimolar exchange with $MgCl_2$. In experiments with increased $[K^+]_o$, KCl was added without osmolarity compensation (in 10.8 mM K^+) or in equimolar exchange with NaCl. Experiments were performed at room temperature (21–23°C). All chemicals were purchased from Sigma Chemical Co. (St. Louis, MO).

Protocols and Parameter Measurements

Two different voltage command protocols were used. Both consisted in a pulse to an initial voltage (V) from a holding potential (H), followed by a pulse to a final voltage (F). In Protocol 1 (e.g., Fig. 3 *A*), V was variable in amplitude and F was constant at −110 mV (distant from the reversal potential of I_{AB}). In Protocol 2 (e.g., Fig. 3 *B*), V was fixed at −130 mV (which clearly activated I_{AB}) and F was variable. The current-voltage (I-V) relationship of the steady state total current evoked by Protocol 1 was measured at the end of V. The instantaneous currents at the beginning of V and F evoked by Protocols 1 and 2, respectively, were measured 7 ms after the pulse transients (when the capacitative currents had ended and the activation and deactivation of I_{AB} were negligible). The instantaneous current at the beginning of V corresponded to the leak current (I_L) and that at the beginning of F corresponded to I_L plus I_{AB} (previously activated by V) (Araque and Buño, 1994). The instantaneous I-V relationships of I_L and $I_L + I_{AB}$, reflected the behavior of the I_L and the open I_{AB} channels, respectively (see Araque and Buño, 1994). The slopes of the calculated linear regressions of both instantaneous I-V relationships corresponded to the chord conductance of I_L (G_L) and to G_L plus the chord conductance of I_{AB} (G_{AB}), respectively. The reversal potential of I_{AB} (E_{AB}) was calculated either from the tail currents evoked by Protocol 2 (see Fig. 4, *B* and *C*) or from the intersect point of the computed linear regressions of the instantaneous I-V relationship of I_L and $I_L + I_{AB}$ (see Araque and Buño, 1994). G_{AB} was calculated from the instantaneous current at the beginning of pulse F in Protocol 1 (see e.g., Fig. 3 *A*), following the equation:

$$G_{AB} = (I - I_{min})/(F - E_{AB}), \quad (1)$$

where I is the instantaneous current at pulse F, which had a minimum (I_{min}) when $G_{AB} = 0$ (see Araque and Buño, 1994). The activation curve of I_{AB}, i.e., the voltage dependence of G_{AB}, was characterized by the expression:

$$G_{AB} = G_{AB,max}/[1 + \exp\{V - Vo)/S\}] \quad (2)$$

deduced from the Boltzmann equation where $G_{AB,max}$ is the maximum G_{AB}, Vo is the voltage at which G_{AB} is half-activated, and S is a slope parameter.

Because leak and capacitive currents were linear (and I_{AB} did not show instantaneous rectification; see Araque and Buño, 1994), they could be adequately subtracted using the pCLAMP software according to the following procedure: the sum of the currents evoked by n identical pulses n-fold smaller than the test pulse was subtracted from the current elicited by

the corresponding test pulse. To prevent significantly activation of voltage-gated currents, n was usually 15.

To minimize the steady state current at the holding potential, H was set near the resting potential (e.g., −60 mV in control solution and −40 mV in 10.8 mM K^+) (see Araque and Buño, 1994). All data were expressed as mean ± SD.

RESULTS

Cd^{2+} Reduction of Both I_{AB} and I_L

Fig. 1 *A* shows total currents evoked by Protocol 1 in control solution, in the presence of 5.0 mM Cd^{2+} and after recovery by washout. In control solution, voltage command

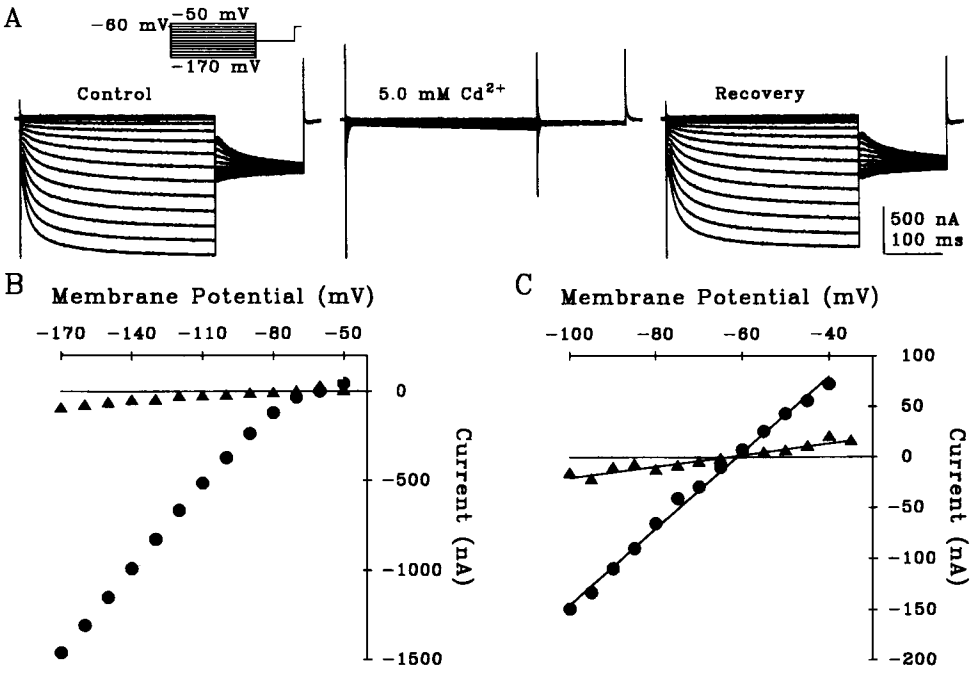

FIGURE 1. I_{AB} was abolished by 5.0 mM Cd^{2+}. (*A*) Total currents in control, 5.0 mM Cd^{2+} and after recovery; voltage command protocol shown above, as in Figs. 2–5. (*B*) *I-V* relationships of steady state total current in control and in 5.0 mM Cd^{2+} (● and ▲, respectively). (*C*) Instantaneous *I-V* relationships of I_L in control and in 5.0 mM Cd^{2+} (● and ▲, respectively) fitted to first-order regressions ($r > 0.95$) (*continuous lines*).

pulses from a holding potential (H) of −60 mV to Vm between −50 and − 170 mV evoked an instantaneous linear leak current I_L. With pulses < -80 mV, I_L was followed by the time- and voltage-dependent inward current I_{AB}. The *I-V* relationships of the steady state total current measured at the end of V clearly shows the inward rectification due to I_{AB} (Fig. 1 *B, circles*). The steady state total current was greatly reduced and its *I-V* relationship became almost linear in 5.0 mM Cd^{2+} solution (Fig. 1 *B, triangles*), indicating that I_{AB} was practically abolished. Further-

more, the instantaneous *I-V* relationship of I_L (Fig. 1 *C*), calculated at the beginning of pulse *V* in Protocol 1 (Fig. 1 *A*), remained linear and the chord conductance G_L (i.e., the first-order regression slope) diminished from 3.7 μS in control to 0.6 μS (i.e., a 83.8% drop) in 5.0 mM Cd^{2+} solution (*circles* and *triangles*, respectively). From eight different preparations, G_L varied from 4.2 ± 0.7 μS in control to 1.5 ± 1.0 μS in 5.0 mM Cd^{2+} solution (i.e., a 64.3% reduction). The reversal potential of I_L (E_L), estimated by linear interpolation of the first-order regression of the instantaneous *I-V*

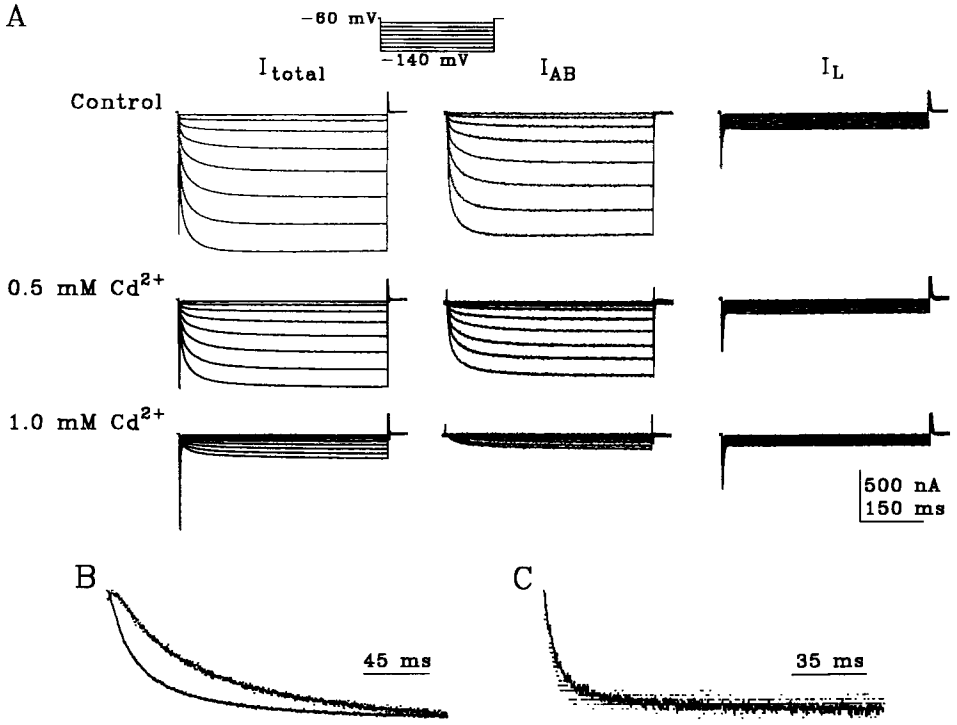

FIGURE 2. Effects of Cd^{2+} on I_{total}, I_{AB}, and I_L. (*A*) I_{total}, I_{AB}, and I_L in control, 0.5 and 1.0 mM Cd^{2+} solutions. I_{AB} was isolated by computer subtraction of linear capacitive and leak currents from total currents. I_L was obtained by computer subtraction of I_{AB} from I_{total}. (*B* and *C*) Activation of I_{AB} elicited by a pulse to −130 mV from a −60-mV holding potential, and deactivation of I_{AB} evoked by a pulse to −60 mV after a prepulse to −130 mV, respectively, in control (*continuous line*) and 0.5 mM Cd^{2+} (*dotted line*). I_{AB} was scaled between minimum and maximum values. *B* and *C* are from the same fiber.

relationship of I_L with the voltage axis (Fig. 1 *C*), was not significantly altered by Cd^{2+}, indicating that the ion did not modify the selective permeability of the channels underlying I_L. Therefore, Cd^{2+} also blocked I_L.

Because I_L was linear (Fig. 1 *C;* see Araque and Buño, 1994), I_{AB} could be isolated by computer substraction of linear current components (capacitive and leak) from the total current (I_{total}), and I_L could be separated by substraction of I_{AB} from I_{total}. Fig. 2 *A* shows I_{total}, I_{AB}, and I_L evoked by hyperpolarizing pulses in control, 0.5 and 1.0

mM Cd^{2+} solutions. Both I_{AB} and I_L were reduced by Cd^{2+} in a dose-dependent manner (see below), but the reduction of I_{AB} was much larger. Furthermore, while the I_{AB} activation kinetic gradually slowed down as a function of the extracellular Cd^{2+} concentration ($[Cd^{2+}]_o$) (Fig. 2 *B;* see also Fig. 8 *C*), the I_{AB} deactivation kinetic was essentially unchanged by Cd^{2+} (Fig. 2 *C*).

Fig. 3, *A* and *B*, shows total currents evoked by Protocol 1 and 2, respectively, in control and 0.5 mM Cd^{2+} solutions. Fig. 3 *C* shows the *I-V* relationships of the steady

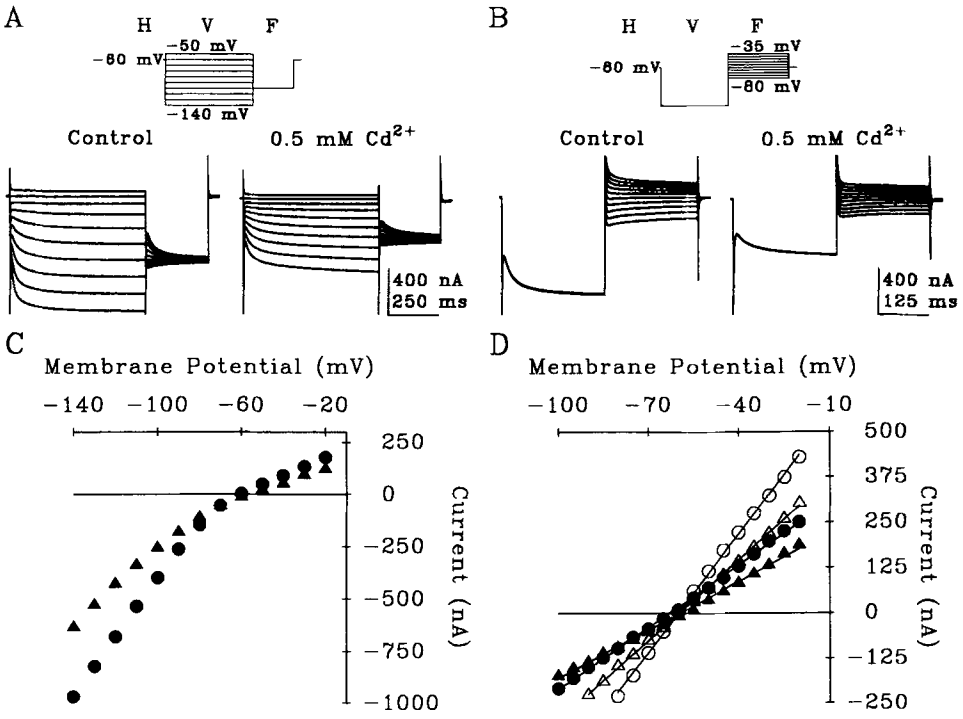

FIGURE 3. I_{AB} was reduced by 0.5 mM Cd^{2+}. (*A* and *B*) Total currents in control and 0.5 mM Cd^{2+}. Voltage command protocols 1 and 2; the holding potential (*H*), first (*V*) and second (*F*) pulses are shown. (*C*) *I-V* relationships of the steady state total current measured at the end of *V* in control (●) and 0.5 mM Cd^{2+} (▲). (*D*) Instantaneous *I-V* relationships of I_L (*filled symbols*) and $I_L + I_{AB}$ (*open symbols*), with (*triangles*) and without (*circles*) 0.5 mM Cd^{2+}, fitted to first-order regressions ($r > 0.99$) (*continuous lines*).

state total current in control and 0.5 mM Cd^{2+} solutions (*circles* and *triangles*, respectively). The steady state total current at *Vm* above −60 mV was reduced in 0.5 mM Cd^{2+}, as expected by the Cd^{2+} blockade of I_L. Furthermore, the nonlinear, inwardly rectifying, *I-V* relationship was maintained in 0.5 mM Cd^{2+} solution, and the reduction of the steady state total current was more prominent at hyperpolarized potentials owing to the addition of the Cd^{2+} inhibition of I_{AB}. Consequently, the Cd^{2+} reduction of I_{AB} was dose dependent, decreasing as $[Cd^{2+}]_o$ decreased (see Fig. 2 and below).

Instantaneous I-V relationships. The instantaneous *I-V* relationships of both I_L and $I_L + I_{AB}$ are shown in Fig. 3 *D*, (*solid* and *open symbols*, respectively). On the one hand, the instantaneous *I-V* relationships of $I_L + I_{AB}$ in control and 0.5 mM Cd^{2+} solutions (*open circles* and *triangles*, respectively) were linear ($r > 0.99$, in both cases), and their slopes (i.e., $G_L + G_{AB}$) varied from 10.9 to 7.4 μS, respectively, (i.e., a 32.1% drop). Furthermore, the linear behavior of the open I_{AB} channels in Cd^{2+} solution indicates that Cd^{2+} did not interfere with the motion of ions through the open I_{AB} channels. Alternatively, Cd^{2+} could unbind slowly from the channel, however, the effects of Cd^{2+} on the kinetic behavior of I_{AB} (see below and Discussion) suggest that the Cd^{2+} binding reaction was faster than the transitions between the open and closed states of I_{AB} channels. On the other hand, G_L in control (*solid circles*) and 0.5 mM Cd^{2+} solutions (*solid triangles*) declined from 5.7 to 4.5 μS, respectively (i.e., a 21.1% drop). On average ($n = 6$), G_L diminished from 4.3 ± 0.8 μS in control to 2.8 ± 1.0 μS (i.e., a 34.9% drop) in 0.5 mM Cd^{2+} solution. Consequently, the Cd^{2+} blockade of I_L was also dose dependent because the G_L drop measured in 5.0 mM Cd^{2+} (see Fig. 1) was much larger than that in 0.5 mM Cd^{2+}.

Reversal potential of I_{AB}. Fig. 4, *A* and *B*, shows total and tail currents evoked by protocol 1 and 2, respectively, in control and 0.5 mM Cd^{2+} solutions. E_{AB} estimated by linear interpolation in the *I-V* relationship of the I_{AB} tail current amplitudes (i.e., the difference between currents at the beginning and end of *F* in protocol 2) was not substantially different in control (−67.6 mV) and 0.5 mM Cd^{2+} (−64.1 mV) solutions (Fig. 4 *C*, *circles* and *triangles*, respectively). The mean E_{AB} in control and 0.5 mM Cd^{2+} solutions ($n = 8$) were −63.8 ± 5.1 and −61.5 ± 7.1 mV, respectively, and they were not significantly different (*t* test; $P > 0.1$), indicating that the selective permeability of the I_{AB} channels was unaffected by Cd^{2+}.

Chord conductance of I_{AB}. Fig. 4 *D* shows the voltage-dependence of G_{AB} (i.e., the I_{AB} activation curve), calculated at the beginning of pulse *F* in protocol 1 (see Fig. 3 *A*), in control and 0.5 mM Cd^{2+} solutions (*circles* and *triangles*, respectively). $G_{AB,max}$ was reduced from 8.6 μS in control to 5.5 μS in 0.5 mM Cd^{2+} solution. Furthermore, the I_{AB} activation curve was shifted by Cd^{2+} to more hyperpolarized potentials, changing *Vo* from −101.6 mV in control to −120.0 mV in 0.5 mM Cd^{2+} solution. However, the slope parameter *S* was only slightly changed (11.2 and 12.8, in control and 0.5 mM Cd^{2+} solutions, respectively). On average ($n = 7$), in 0.5 mM Cd^{2+} solution $G_{AB,max}$ was reduced 0.52 ± 0.27 times, *Vo* was displaced −14.7 ± 6.7 mV and *S* was changed 0.7 ± 1.6 U from the control solution (see Fig. 7).

Therefore, Cd^{2+} reduced G_{AB} and shifted the I_{AB} activation curve to hyperpolarized potentials, suggesting that it acted as a modifier of gating (see below). Furthermore, Cd^{2+} did not modify the slope parameter *S* (which defines the shape of the Boltzmann relation), i.e., if scaled and shifted, the activation curves in the presence and absence of Cd^{2+} could be superimposed (not shown), indicating that the same relative amount of channels were opened by a given *Vm* increment.

Kinetic behavior of I_{AB}. The kinetic behavior of I_{AB} was also affected by Cd^{2+} (see Fig. 2). Although the characterization of the I_{AB} time course by more than a single exponential function cannot be discarded, the time course of both I_{AB} activation and deactivation (Fig. 4, *A* and *B*, *dotted lines*) could be reasonably fitted ($r > 0.95$) by single-exponential functions (*continuous lines*) and both kinetics could be described by

a single time constant (τ_{AB}), which for convenience corresponded to the activation time constant at $Vm < -80$ mV and to the deactivation time constant at the remaining Vm (see Araque and Buño, 1994). Furthermore, the voltage dependence of τ_{AB} (i.e., the τ_{AB}-Vm relationship) was a bell-shaped function with a peak at $\sim Vo$ (Araque and Buño, 1994). Fig. 4 *E* displays the τ_{AB}-Vm relationships in control (*circles*) and 0.5 mM Cd^{2+} (*triangles*) solutions, showing the shift to the left on the voltage axis produced by Cd^{2+} (responsible for the similar I_{AB} activation curve shift; see Fig. 4 *D*). Moreover, while the magnitude of the deactivation τ_{AB} was not modified (note that

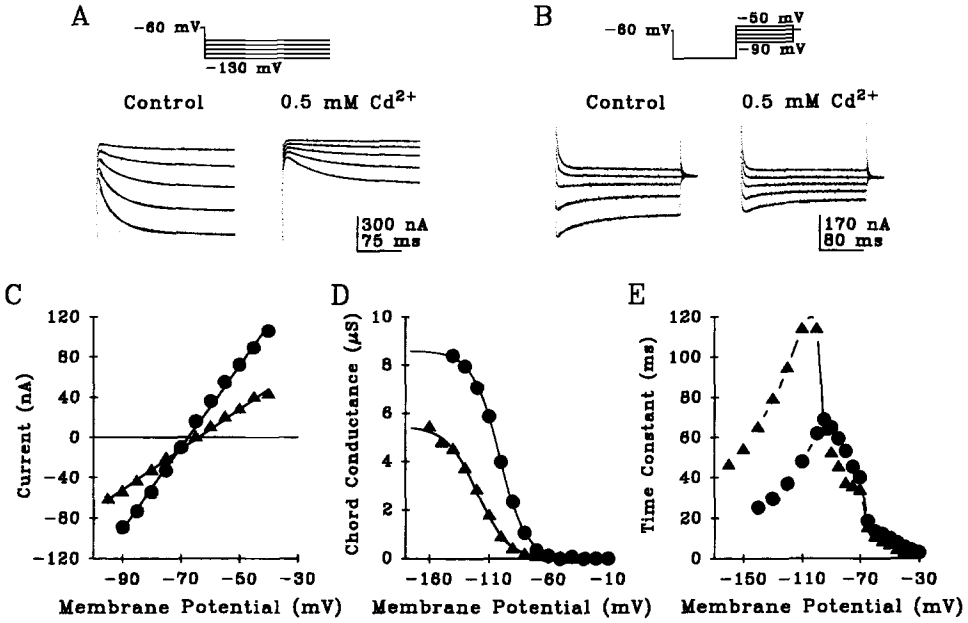

FIGURE 4. E_{AB}, G_{AB}, and τ_{AB} in control and 0.5 mM Cd^{2+}. (*A* and *B*) Total currents (*dots*) evoked by *V* and *F* pulses in Protocols 1 and 2, respectively, in control and in 0.5 mM Cd^{2+}. Superimposed continuous lines are single-exponential fits ($r > 0.95$) to each record. (*C*) *I-V* relationships of I_{AB} tail current amplitudes in control and 0.5 mM Cd^{2+} (● and ▲, respectively) fitted to first-order regressions ($r > 0.99$) (*continuous lines*). (*D*) Voltage dependence of G_{AB} in control (●) and 0.5 mM Cd^{2+} (▲). G_{AB} was calculated from Eq. 1 and fitted to Eq. 2 (*continuous lines*) (see Materials and Methods). In control: $G_{AB,max} = 8.6 \pm 0.1$ μS, $Vo = -101.6 \pm 0.4$ mV and $S = 11.2 \pm 0.3$; in 0.5 mM Cd^{2+}: $G_{AB,max} = 5.5 \pm 0.1$ μS, $Vo = -120.0 \pm 0.9$ mV and $S = 12.8 \pm 0.6$. (*E*) τ_{AB}-Vm relationships in control (●) and 0.5 mM Cd^{2+} (▲).

the apparent decrease corresponded to the I_{AB} activation curve shift), the magnitude of the activation τ_{AB} was markedly augmented in 0.5 mM Cd^{2+} solution, and this increment was dependent on the $[Cd^{2+}]_o$ (see Fig. 8 *C*). In conclusion, the time course of I_{AB} in the presence of Cd^{2+} remained a single exponential function, the deactivation rate of I_{AB} was unchanged and the I_{AB} activation was slowed by Cd^{2+}. These results suggest that Cd^{2+} bound and unbound faster than the transitions between closed and open states of I_{AB} channels (see Discussion) and that Cd^{2+} acted on the gating mechanism involved in the opening of I_{AB} channels.

Intracellular Cd^{2+}

In four experiments, the current electrode was substituted after a control recording by a new electrode filled with 1M $CdCl_2$. Cd^{2+} was ionophoretically injected with 80 ms, 50-nA current pulses, delivered at 1/s during 30–60 min. Both I_L and I_{AB} were unmodified by intracellular injection of Cd^{2+} (not shown). The amount of Cd^{2+} ionophoresed was estimated from the equation (Adler, Augustine, Duffy, and Charlton, 1991):

$$n = ItT_b/Fz$$

where n is the number of moles injected, I is the injected current intensity, T_b is the transference number (i.e., the fraction of current carried by Cd^{2+}), F is Faraday's constant, and z is the ion's valence. Assuming that Cd^{2+} has the same electric mobility than Mg^{2+}, T_b would be 0.41 (Hille, 1992). If all the injected Cd^{2+} stayed inside the cell and considering a standard muscle fiber volume of 3.14 nl (length, 400 μm; diam, 100 μm), the estimated intracellular Cd^{2+} concentration varied between 4.87 and 9.74 mM. The negative result of Cd^{2+} injection indicates that the effects of extracellular Cd^{2+} were not due to leak of Cd^{2+} into the cell through electrode penetrations, which could act from the inside at micromalar levels. Therefore, Cd^{2+} acted by binding to a receptor site in the extracellular side of the membrane.

Cd^{2+} Regulation of I_{AB} in Different $[K^+]_o$

The above results indicate that the selective permeability of the I_{AB} channels was not affected by Cd^{2+}, and that Cd^{2+} acted from the extracellular side. It has been proposed that a permeant ion must bind to at least one site in the permeation pathway when migrating through a channel (Hess and Tsien, 1984; Hess, Lansman, and Tsien, 1986). Thus, ionic pore occluders and permeant ions usually compete for common binding sites at the channel (e.g., Standen and Stanfield, 1978; Mlinar and Enyeart, 1993; see also Lester, 1991; Hille, 1992), although the blocker could also occlude the pore at a peripheral site far away of the permeation pathway.

To explore whether Cd^{2+} exerted its effects by binding to a site involved in the K^+ permeability pathway, the effects of Cd^{2+} in different $[K^+]_o$ were analyzed. Fig. 5, *A* and *B*, shows total currents in 5.4 and 10.8 mM K^+ solutions, respectively, in the absence (*top*) and the presence of 0.5 mM Cd^{2+} (*bottom*). The Cd^{2+}-induced current reduction is evident in both $[K^+]_o$. Fig. 5 *C*, shows the corresponding *I-V* relationships of the steady state total current in 5.4 and 10.8 mM K^+ (*solid and open symbols*, respectively), without (*circles*) and with 0.5 mM Cd^{2+} (*triangles*). It had previously been shown that the *I-V* relationship of the steady state total current shifted 58 mV towards positive potentials by a 10-fold increase in $[K^+]_o$ (Araque and Buño, 1994). In accordance with the shift, the *I-V* relationship of the steady state total current in raised $[K^+]_o$ was similarly displaced ~17 mV to the right both in the absence and the presence of 0.5 mM Cd^{2+}. Moreover, the degree of Cd^{2+} reduction in 5.4 and 10.8 mM K^+ was 55 and 56%, respectively (measured at −120 and −140 mV, respectively). Consequently, the Cd^{2+} reduction was similar irrespective of the *I-V* shift and of $[K^+]_o$.

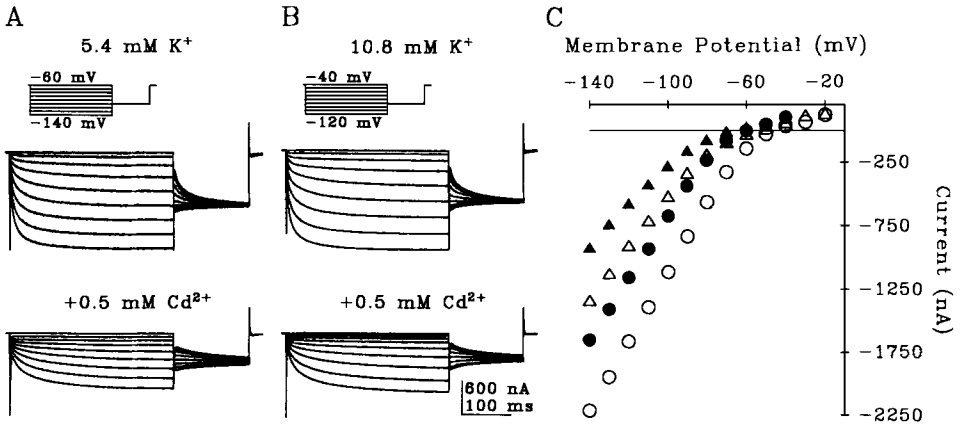

FIGURE 5. Cd^{2+} blockade of I_{AB} was independent of $[K^+]_o$. (*A* and *B*) Total currents in 5.4 and 10.8 mM K^+, respectively, in the absence (*top*) and presence (*bottom*) of 0.5 mM Cd^{2+}. (*C*) *I-V* relationships of the steady state total current in 5.4 and 10.8 mM K^+ (*solid and open symbols*, respectively), in the absence and presence of 0.5 mM Cd^{2+} (*circles and triangles*, respectively).

Reversal potential of I_{AB}. Fig. 6 *A* shows the *I-V* relationship of the I_{AB} tail current amplitudes evoked by protocol 2. E_{AB} shifted to more depolarized *Vm* in high $[K^+]_o$, and the corresponding E_{AB} in 5.4 and 10.8 mM K^+ (*solid and open symbols*) were not modified by Cd^{2+} (*triangles*), again indicating that the selective permeability of the I_{AB} channels was unaffected by Cd^{2+}.

Chord conductance of I_{AB}. Fig. 6 *B* shows the voltage dependence of G_{AB} in 5.4 and 10.8 mM K^+ solutions (*solid and open symbols*, respectively) and in the absence and

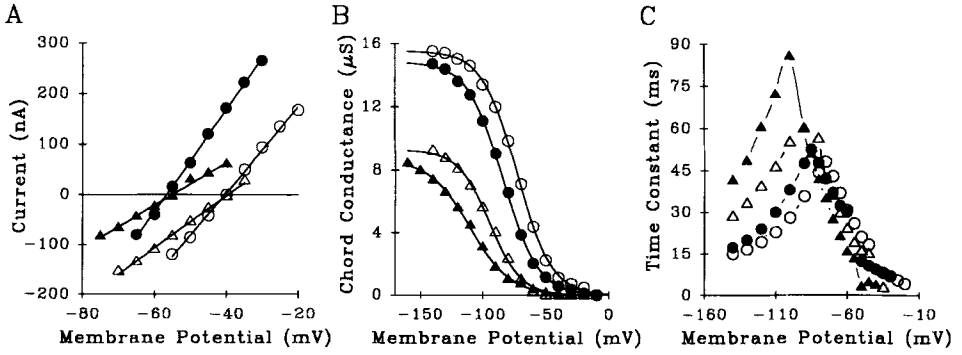

FIGURE 6. Effects of Cd^{2+} on E_{AB}, G_{AB}, and τ_{AB} in different $[K^+]_o$. Effects of 5.4 and 10.8 mM K^+ (*solid and open symbols*, respectively) without and with 0.5 mM Cd^{2+} (*circles and triangles*, respectively). Same fiber of Fig. 5. (*A*) *I-V* relationships of I_{AB} tail current amplitudes, fitted to first-order regressions ($r > 0.99$) (*continuous lines*). (*B*) Voltage dependence of G_{AB}, calculated from Eq. 1 and fitted to Eq. 2 (*continuous lines*) (see Materials and Methods). In control, in 5.4 mM K^+: $G_{AB,max} = 14.8 \pm 0.1$ μS, $Vo = -84.1 \pm 0.4$ mV and $S = 13.9 \pm 0.3$; in 10.8 mM K^+: $G_{AB,max} = 15.5 \pm 0.1$ μS, $Vo = -72.9 \pm 0.4$ mV and $S = 13.7 \pm 0.3$. In 0.5 mM Cd^{2+}, in 5.4 mM K^+: $G_{AB,max} = 8.7 \pm 0.1$ μS, $Vo = -110.3 \pm 0.8$ mV and $S = 16.0 \pm 0.5$; in 10.8 mM K^+: $G_{AB,max} = 9.3 \pm 0.2$ μS, $Vo = -94.8 \pm 0.9$ mV and $S = 12.4 \pm 0.7$. (*C*) τ_{AB}-*Vm* relationships.

the presence of 0.5 mM Cd^{2+} (*circles and triangles,* respectively). $G_{AB,max}$ was similarly reduced by Cd^{2+} in both $[K^+]_o$, i.e., to 58.8 and 60.0% (see also Fig. 7 *A* and below). Araque and Buño (1994) described that the activation curve of I_{AB} shifted towards positive *Vm* by ~58 mV with a 10-fold increase in $[K^+]_o$ (Fig. 6 *B, circles*). The voltage dependence of G_{AB} was shifted to more negative potentials in the presence of Cd^{2+}, and the shift was similar in both $[K^+]_o$ (−26.2 and −21.9 mV in 5.4 and 10.8 mM K^+ solutions), while the slope parameter *S* was, if any, slightly changed (Fig. 6 *B*). Indeed, on average *Vo* changed −14.7 ± 6.7 mV ($n = 7$) and −20.1 ± 3.9 mV ($n = 6$) by 0.5 mM Cd^{2+} in 5.4 and 10.8 mM K^+ solutions, respectively, and the difference between *S* with and without 0.5 mM Cd^{2+} was 0.7 ± 1.6 and 0.1 ± 2.0 in 5.4 and 10.8 mM K^+ solutions, respectively. Therefore, the Cd^{2+} regulation was not affected by $[K^+]_o$, suggesting that Cd^{2+} did not exert its effect by binding to a site involved in the K^+ permeability pathway.

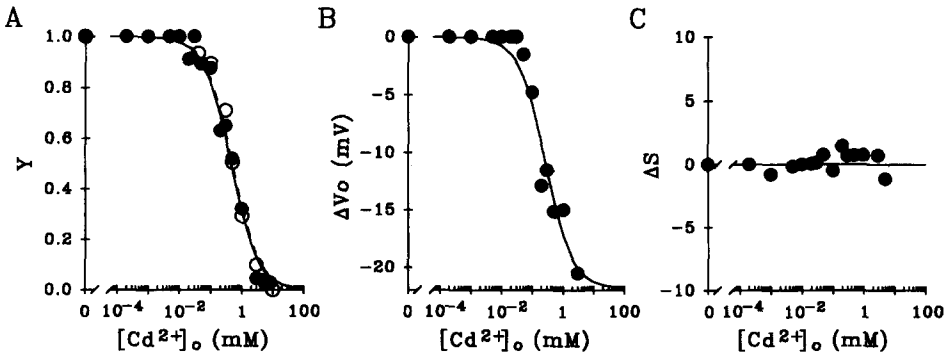

FIGURE 7. Concentration-effect curves of $[Cd^{2+}]_o$ on $G_{AB,max}$, *Vo* and *S* (see Materials and Methods, Eq. 2). (*A*) Ratio (*Y*) between $G_{AB,max}$ in Cd^{2+} and in control solution, in 5.4 and 10.8 mM K^+ (*filled and open circles,* respectively) fitted to Eq. 3 (*continuous and dashed lines,* respectively) (see Results). (*B*) Differences (ΔVo) between *Vo* in Cd^{2+} and in control solution, fitted to Eq. 4 (*continuous line*) (see Results). (*C*) Differences (ΔS) between the slope parameter *S* in Cd^{2+} and in control solution. All experimental values are means from at least six different preparations.

Kinetic behavior of I_{AB}. Fig. 6 *C* shows the τ_{AB}-*Vm* relationship in 5.4 and 10.8 mM K^+ solutions (*solid and open symbols,* respectively) in the absence and presence of 0.5 mM Cd^{2+} (*circles and triangles,* respectively). The voltage dependence of τ_{AB} was shifted to more depolarized potentials in raised $[K^+]_o$, as expected by the I_{AB} activation curve shift. Furthermore, in 0.5 mM Cd^{2+}, the τ_{AB}-*Vm* relationship was shifted to the left (Fig. 6 *C, triangles*), also in accordance with the similar I_{AB} activation curve shift (see above, and Fig. 6 *B*). However, the effects of Cd^{2+} on the τ_{AB}-*Vm* relationships were similar in both $[K^+]_o$, i.e., the shift to the left was the same, the deactivation rate of I_{AB} was unchanged, and the activation τ_{AB} was similarly augmented by Cd^{2+} in both $[K^+]_o$. Indeed, the activation τ_{AB} increased ~1.5 and 1.4 times in 5.4 and 10.8 mM K^+, respectively, at potentials ~30 mV more hyperpolarized than the corresponding *Vo*.

We were not able to perform similar studies using very high $[K^+]_o$ because G_L increased (>30 μS in 100 mM K^+) preventing accurate recordings (see Araque and Buño, 1994). However, a solution containing 100 mM K^+ plus 10 mM Cd^{2+} (which reduced G_L below 15 μS) was used. In these conditions, I_{AB} was absent in all the seven fibers tested (not shown), indicating that a high $[K^+]_o$ did not remove the effect of Cd^{2+}.

Therefore, because the Cd^{2+}-regulation was unaffected by $[K^+]_o$, we conclude that Cd^{2+} did not compete with K^+ for its binding site to modulate I_{AB} channels, again supporting that Cd^{2+} did not exert its effect by binding to a site in the K^+ permeability pathway.

Dose Dependence of Cd^{2+} Regulation of I_{AB}

Results described so far show that as $[Cd^{2+}]_o$ increased, $G_{AB,max}$ was reduced and the I_{AB} activation curve was shifted towards more negative *Vm* in a dose-dependent manner. Results obtained from 19 different preparations displaying the effects of $[Cd^{2+}]_o$ on G_{AB} and its voltage dependence are shown in Fig. 7. The Cd^{2+} concentration-effect relationships on $G_{AB,max}$ (i.e., the degree of reduction as a function of $[Cd^{2+}]_o$) in 5.4 and 10.8 mM K^+ are shown in Fig. 7 *A* (*filled and open circles,* respectively). Mean values of the ratio (*Y*) between $G_{AB,max}$ in Cd^{2+} and in control solutions were fitted to the equation:

$$Y = Y_{max}/[1 + (Cd/IC_{50})^1] \quad (3)$$

deduced from the Hill equation, where Y_{max} is the maximum *Y*, *Cd* is $[Cd^{2+}]_o$, IC_{50} is the $[Cd^{2+}]_o$ at which $Y = ½\ Y_{max}$ and the Hill coefficient, i.e., the exponential value is 1. The fit statistics ($r > 0.99$, in both cases) indicate that the effect of $[Cd^{2+}]_o$ on G_{AB} was dose dependent, increasing as $[Cd^{2+}]_o$ increased and obeying the Hill equation with a Hill coefficient of 1, supporting the assumption of 1:1 ligand:receptor binding. Furthermore, the fit parameters of IC_{50} in 5.4 and 10.8 mM K^+ were 0.452 ± 0.045 and 0.495 ± 0.080 mM, respectively, which were not significantly different (*t* test; $P > 0.1$), again indicating that the Cd^{2+} regulation was unaffected by $[K^+]_o$, and that Cd^{2+} did not exert its action by binding to a site involved in the K^+ permeability pathway.

The I_{AB} activation curve shift evoked by Cd^{2+} was estimated by the effect of $[Cd^{2+}]_o$ on *Vo* (Fig. 7 *B*). The mean differences between *Vo* in Cd^{2+} and in control solutions (ΔVo) were plotted versus $[Cd^{2+}]_o$. Since at $[Cd^{2+}]_o > 5.0$ mM, G_{AB} was drastically reduced and could not be successfully fitted to the Boltzmann equation, a saturation of ΔVo at high $[Cd^{2+}]_o$ could not be found. Moreover, when $G_{AB,max} = 0$, *Vo* is mathematically undetermined. However, attempts were made to fit experimental values to the expression:

$$\Delta Vo = \Delta Vo_{min} - [\Delta Vo_{min}/\{1 + (Cd/IC_{50})^1\}] \quad (4)$$

also deduced from the Hill equation, assuming a Hill coefficient of 1 and where ΔVo_{min} is the minimum value of ΔVo. The procedure provided a reasonable fit ($r > 0.95$), again supporting the assumption of 1:1 Cd^{2+} binding. Furthermore, the concentration-effect relationship on *Vo* was similar to that on $G_{AB,max}$. Indeed, the

relationship between ΔVo and Y was linear ($r > 0.95$; not shown), suggesting that the Cd^{2+}-evoked G_{AB} reduction and the shift in G_{AB} voltage dependence were due to the same mechanism.

The mean differences between the slope parameter S in Cd^{2+} and in control solutions (ΔS) versus $[Cd^{2+}]_o$ are shown in Fig. 7 *C*. No meaningful differences (*t* test; $P > 0.1$) were found between the mean ΔS in control and in different $[Cd^{2+}]_o$ solutions. Indeed, the correlation coefficient between ΔS and $[Cd^{2+}]_o$ was not significantly different from zero.

DISCUSSION

Our results show that both I_{AB} and I_L were reduced by low extracellular concentrations of Cd^{2+} in a dose-dependent manner.

Cd^{2+} Regulation of I_{AB}

The Cd^{2+} regulation had the following characteristics: (*a*) E_{AB} was not modified, indicating that the I_{AB} reduction was not caused by interfering with the channel's selective permeability mechanisms; (*b*) Cd^{2+} did not compete with K^+ for the regulatory site, suggesting that Cd^{2+} did not bind to the site for K^+ in the permeation pathway; (*c*) the regulation did not modify the slope parameter S of the I_{AB} voltage dependence; (*d*) the voltage dependence of G_{AB} was shifted to more hyperpolarized potentials; (*e*) the activation τ_{AB} was increased but the magnitude of the deactivation time constant was unaffected.

Therefore, many aspects of the regulation of G_{AB} by Cd^{2+} were different from that of other anomalous rectifiers blocked by different ions. For example, Cs^+ blocked all other known inward rectifiers in a voltage-dependent manner (e.g., Gay and Stanfield, 1977; Mayer and Westbrook, 1983). Voltage-dependent block by different ions has also been described in many conductances (e.g., Lansman et al., 1986; Swandulla and Armstrong, 1989; Lansman, 1990). On the one hand, it has been suggested that nonpermeant positively charged blocking ions bind to the channel attracted by the increased transmembrane electrical field during hyperpolarization and that depolarization disengages the blocking ion (Woodhull, 1973; Gay and Stanfield, 1977; Standen and Stanfield, 1978). This is not the case for I_{AB} because the open channel behavior was linear in the presence of Cd^{2+} for the voltage range studied, which appears large enough in the depolarizing direction. On the other hand, extreme hyperpolarization could force the blocking cation to permeate through the channel, also alleviating block. This is clearly not the case for Cd^{2+} regulation of I_{AB} which was not relieved by strong hyperpolarizations to -170 mV (see below). It has been shown that Ba^{2+} blocked the inward rectifier of frog skeletal muscle by competing with K^+ for a site in the K^+ permeability pathway (Standen and Stanfield, 1978). However, Cd^{2+} did not compete with K^+ for its blocking site. These results suggest a different mode of action of Cd^{2+}, which acted by binding to a receptor site outside the K^+ permeability pathway. Cd^{2+} could occlude the pore by binding to an external site away from the K^+ permeability pathway and, because the instantaneous *I-V* relationship of I_{AB} remained linear in the presence of Cd^{2+},

binding could occur outside the membrane electric field (perhaps in the outer vestibule of the channel). However, the effects of Cd^{2+} on both the activation curve and the time course of I_{AB} strongly favor the interpretation that Cd^{2+} affected the gating mechanism of I_{AB} channels (see below) rather than Cd^{2+} acted by ionic pore occlusion.

Frankenhaeuser and Hodgkin (1957) described that changes in $[Ca^{2+}]_o$ shifted the voltage dependence of Na^+ and K^+ currents in squid axons and proposed that Ca^{2+} interacted with surface negative charges creating an electric field inside the membrane which adds to the resting potential. Due to that effect, the voltage dependence of most voltage-gated currents was shifted towards positive *Vm* in raised extracellular divalent cation concentrations (an effect termed, screening). Interestingly, inward rectifiers and hyperpolarization-activated currents did not show screening (Hille, 1992). Moreover, the Cd^{2+}-evoked shift of the G_{AB} voltage dependence was towards negative potentials, indicating that Cd^{2+} effects cannot be explained by screening, since in that case a positive shift would occur. Furthermore, the extracellular concentration of divalent cations was maintained constant by equimolar replacement with Mg^{2+}, and the reduction of G_{AB} was not reproduced by Mn^{2+} or Ba^{2+} (see Araque and Buño, 1994).

The channel gating properties are defined by the conductance-*Vm* relationship and by the opening and closing time course of the channels (i.e., the τ-*Vm* relationships) (cf, Gilly and Armstrong, 1982: Armstrong and López-Barneo, 1987; Edman and Grampp, 1989; Swandulla and Armstrong, 1989; Ganfornina and López-Barneo, 1992; Hille, 1992). As discussed above, Cd^{2+} modified the voltage dependence of G_{AB}, shifting the activation curve to hyperpolarized levels without affecting the slope parameter *S*. This result strongly suggests that Cd^{2+} acted by modifying the gating properties of I_{AB} channels. Furthermore, the activation τ_{AB} was increased by Cd^{2+}, again indicating that gating mechanisms involved in opening I_{AB} channels were modified by Cd^{2+}. Contrastingly, the deactivation τ_{AB}, i.e., the closing time course of I_{AB} channels, was unaffected by Cd^{2+}, indicating that the gating mechanisms engaged in channel deactivation were not modified.

The above interpretations were incorporated into a kinetic scheme which supplies additional information on the mechanism of the Cd^{2+} regulation. Assuming an ohmic open channel with an intrinsic gating mechanism (see above and Araque and Buño, 1994), the simplest representation with the minimal conformational states to explain the voltage dependence and kinetic of I_{AB} is a two-state model like that proposed by Chesnoy-Marchais (1983) to explain Cl^--mediated inward rectification in *Aplysia* neurons (see also Araque and Buño, 1994). Thus, the voltage dependence of G_{AB} and τ_{AB} could be explained supposing that I_{AB} channels may be in a conducting or open state (O) with a voltage-independent conductance (because the instantaneous *I-V* relationship of I_{AB} was linear), or in a nonconducting or closed state (*C*), with voltage-dependent transition rates (α and β) between both states:

$$C \underset{\beta}{\overset{\alpha}{\rightleftharpoons}} O$$

Following this model, G_{AB} and τ_{AB} are given by the equations:

$$G_{AB} = G_{AB,max}[\alpha/(\alpha + \beta)] \quad (5)$$

$$\tau_{AB} = 1/(\alpha + \beta). \quad (6)$$

To test the accuracy of the model in describing the voltage and time dependence of I_{AB}, α and β were deduced from the above equations (see Chesnoy-Marchais, 1983). They could be considered as exponential functions of *Vm*, and were accurately fitted ($r > 0.95$) to the expressions:

$$\alpha = \alpha_0 \exp(-aVm) \quad (7)$$

$$\beta = \beta_0 \exp(bVm) \quad (8)$$

were α_0, β_0, a, and b were constants. Fig. 8, *E* and *F* (*circles*), shows an example illustrating that the model accurately described the I_{AB} behavior. Mean values obtained from six different experiments for α_0, β_0, a and b were 1.2 ± 0.6 s^{-1}, 962.6 ± 749.7 s^{-1}, 25.9 ± 5.7 V^{-1} and 50.3 ± 12.5 V^{-1}, respectively.

Because the time course of I_{AB} in the presence of Cd^{2+} remained a single exponential function, the deactivation I_{AB} was unchanged and the I_{AB} activation was slowed down by Cd^{2+}, Cd^{2+} would bind faster than the transitions between closed and open states of the I_{AB} channels. In addition, Cd^{2+} did not act by ionic pore occlusion by binding to the open I_{AB} channel (see above). Therefore, while a C-O-B model could be probably excluded, the effects of Cd^{2+} on I_{AB} were reasonably explained by a B-C-O model. Although a more complex scheme with more conformational states (see, e.g., Ganfornina and López-Barneo, 1992) could be proposed, the simplest kinetic model including the minimal conformational states required to explain the voltage dependence and kinetics of I_{AB} and the effects of Cd^{2+} is shown in Fig. 8 *A*. In the model, CB and OB are Cd^{2+}-bound channel states that cannot conduct, K and K' are affinity constants for Cd^{2+} and α, β, and α' are transition rate constants. Because the magnitude of the deactivation τ_{AB} was unchanged by Cd^{2+}, β was assumed as unmodified by Cd^{2+}. Cd^{2+} would slow down the I_{AB} channel opening by decreasing the rate constant α by a factor f (< 1), i.e., $\alpha' = \alpha f$. For microscopic reversibility, Cd^{2+} must bind with lower affinity to the open state, i.e., $K' = Kf$ (see Katz and Thesleff, 1957).

The model predicts that the activation and deactivation of I_{AB} can be described by single exponential functions (only if Cd^{2+} binding is much faster than the gating of I_{AB} channels), and that Cd^{2+} decreases $G_{AB,max}$ and shifts the I_{AB} activation curve to hyperpolarized potentials (given the voltage dependence of α and β and the voltage independence of K and K'), as we found experimentally. The reduction in $G_{AB,max}$ at negative voltages would rule out a pure B-C-O model, since this model also predicts that the effect of Cd^{2+} could be overcome at sufficiently negative voltages. Nevertheless, we cannot confirm this prediction experimentally because strong hyperpolarizations (usually > -140 mV) evoked a large, slow, long-lasting inward current which has not been identified (see Araque and Buño, 1994) and which may mask I_{AB}. However, the observed dose-dependent reduction of $G_{AB,max}$ by Cd^{2+} implies a significant contribution of the rightmost equilibrium. Therefore, Eq. 5 for G_{AB} in

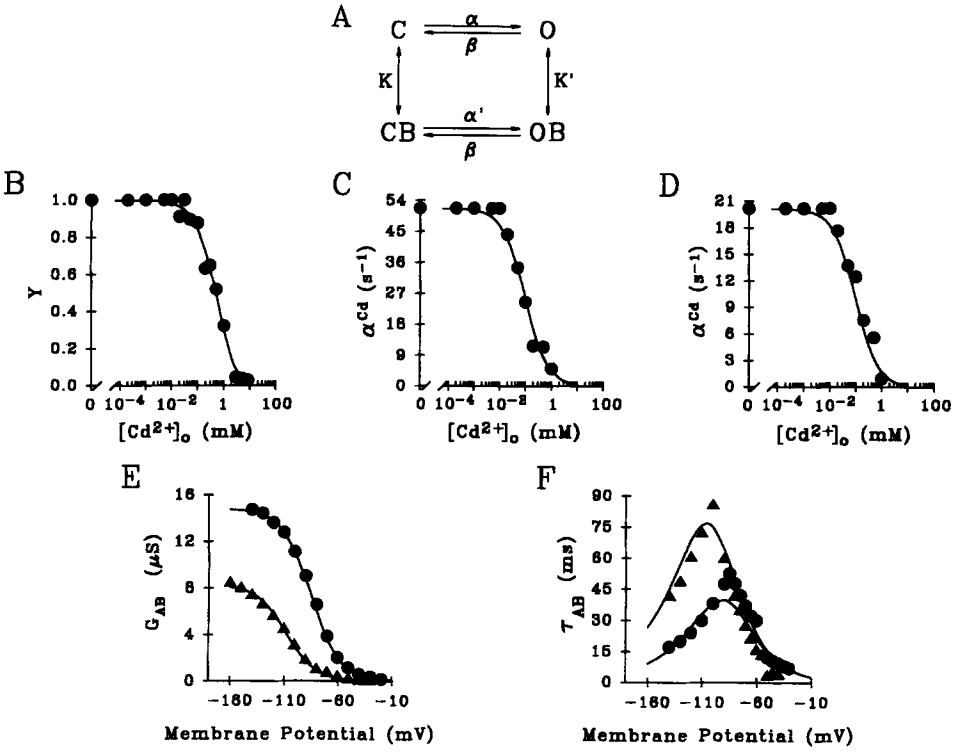

FIGURE 8. Kinetic model of Cd^{2+} effects on I_{AB} gating. (*A*) State diagram of the I_{AB} channel in the presence of Cd^{2+} (see Discussion). (*B*) Ratio (*Y*) between $G_{AB,max}$ in Cd^{2+} and in control solution (n = 10). The continuous line corresponds to Eq. 12, where α = 52.1 s^{-1} and β = 0.7 s^{-1}. Fitting parameters: K' = 1.5 ± 0.2 mM^{-1} and K = 11.6 ± 1.7 mM^{-1}. (*C*) Mean (n = 10) activation rate constant at *Vm* between −130 and −150 mV $[Cd^{2+}]_o$. The continuous line is given by Eq. 11, where α = 52.1 s^{-1} and K = 11.6 mM^{-1}. (*D*) Mean (n = 10) activation rate constant at −100 mV $[Cd^{2+}]_o$. The continuous line is the solution of Eq. 11, with α = 20.1 s^{-1} and K = 11.6 mM^{-1}. In *B* to *D*, α and β were mean values (n = 6) determined from Eqs. 5–8, at *Vm* = −145 mV (*B* and *C*) and *Vm* = −100 mV (*D*). (*E*) Voltage dependence of G_{AB} in control (●) and 0.5 mM Cd^{2+} (▲) solutions. The continuous line for the control solution is given by Eq. 5, where $G_{AB,max}$ = 14.8 μS. Experimental values in Cd^{2+} solution are fitted to Eq. 9. Fitting parameters were: K' = 1.6 ± 0.1 mM^{-1} and K = 8.5 ± 0.5 mM^{-1}. (*F*) τ_{AB}*en Vm* relationships in control and 0.5 mM Cd^{2+} solutions (● and ▲, respectively). The continuous lines correspond to Eqs. 6 and 10, for control and Cd^{2+} solutions, respectively, where K' = 1.6 mM^{-1} and K = 8.5 mM^{-1}. In *E* and *F* (same fiber), α and β were deduced from Eqs. 5–8, where α_0, β_0, *a* and *b* were 1.1 s^{-1}, 582.5 s^{-1}, 28.4 V^{-1} and 44.9 V^{-1}, respectively.

Cd^{2+} could be rewritten as:

$$G_{AB} = [G_{AB,max}/(1 + K'Cd)][\alpha^{Cd}/\alpha^{Cd} + \beta)] \quad (9)$$

where *Cd* is $[Cd^{2+}]_o$ and α^{Cd} is the over-all transition rate constant, which is a function of α and $[Cd^{2+}]_o$ (see below), and that is equal to α in the absence of Cd^{2+}. According

to Katz and Thesleff (1957), the over-all time constant to reach the equilibrium would be given by the equation:

$$\tau_{AB} = 1/[\{\alpha(1 + K'Cd)/(1 + KCd)\} + \beta] \quad (10)$$

thus, from Eqs. 5 and 6, and Eqs. 9 and 10, α^{Cd} should be:

$$\alpha^{Cd} = \alpha/(1 + KCd). \quad (11)$$

From Eqs. 5 and 9, the dose-dependent reduction of G_{AB} would be given by the equation:

$$Y = [1/(1 + K'Cd)][(\alpha + \beta)/\{\alpha + \beta(1 + KCd)\}] \quad (12)$$

Fig. 8 *B* shows that experimental values could be accurately fitted to Eq. 12, where fitting parameters were: $K' = 1.5 \pm 0.2$ mM^{-1} and $K = 11.6 \pm 1.7$ mM^{-1}.

The dose-dependent reduction of α^{Cd} is shown in Fig. 8 *C*, where mean values of the activation rate constant of I_{AB} (obtained from Eqs. 5–8, from 10 different experiments at *Vm* between −130 and −150 mV) were plotted vs $[Cd^{2+}]_o$ (Fig. 8 *C*, *circles*). The model, i.e., the solution of Eq. 11 (where K took the value obtained for the dose-dependent reduction of G_{AB}), accurately described the Cd^{2+}-induced activation rate constant modification (Fig. 8 *C*, *continuous line*). Indeed, values could also be accurately fitted to Eq. 11 (not shown), where the fitting parameter K was 10.4 ± 1.1 mM^{-1}, which was not significantly different from that obtained for the dose-dependent reduction of G_{AB} (*t* test; $P > 0.1$).

The adequate fit of the model to the experimental data was also analyzed by comparing the experimental data with the predicted Cd^{2+} effects on the activation rate constant of I_{AB} at different *Vm*. Fig. 8 *D* shows the relationship between the activation rate constant at −100 mV and $[Cd^{2+}]_o$. The solution of Eq. 11 (where $K = 11.6$ mM^{-1}) (*continuous line*) was in good agreement with the experimental data (*circles;* mean values from 10 experiments).

The adequate match of the model was further evaluated by comparing the modeled predictions of Cd^{2+} effects on the voltage dependence of G_{AB} and on the time dependence of I_{AB}. A representative example is showed in Fig. 8, *E* and *F*. The I_{AB} activation curve in control and 0.5 mM Cd^{2+} solutions are displayed in Fig. 8 *E* (*circles and triangles,* respectively). The theoretical curve for the control solution was obtained from Eq. 5, and the experimental values in Cd^{2+} solution were fitted to Eq. 9, where fitting parameters were: $K' = 1.6 \pm 0.1$ mM^{-1} and $K = 8.5 \pm 0.5$ mM^{-1} (which were acceptably close to those obtained from mean values of Fig. 8, *B* and *C*). The τ_{AB}-*Vm* relationships in control and in 0.5 mM Cd^{2+} solutions are shown in Fig. 8 *F*. The theoretical curve for the control solution was obtained from Eq. 6. For 0.5 mM Cd^{2+}, the solution of Eq. 10 (*continuous line*) (where K and K' took the values obtained for the I_{AB} activation curve) reproduced acceptably well the experimental values. Hence, the model also reproduced quantitatively the Cd^{2+}-effects on G_{AB}, the I_{AB} activation curve, and the kinetic behavior of I_{AB}.

Therefore, this simple kinetic model explains how Cd^{2+} can reduce G_{AB}, slow down the activation kinetic of I_{AB} without affecting the I_{AB} deactivation rate, and shift the current's voltage-dependence to negative *Vm*.

A similar effect was described by Gilly and Armstrong (1982) in squid axon where Zn^{2+} slowed down the Na^+ channel activation but not its deactivation. After their interpretation, we suggest that Cd^{2+} would be attracted by a negatively charged component of the gating apparatus. The binding of Cd^{2+} would stabilize the gating apparatus at its resting position, increasing the energy barrier for the transition from the closed to the open channel states, thus, decreasing the activation rate constant and slowing down the activation of the I_{AB} channels. Accordingly, the energy barrier for the transition from the open to the closed channel states, and therefore the deactivation rate β, would be unaffected since Cd^{2+} had drifted away during activation. Therefore, we conclude that Cd^{2+} acted by interfering with the gating mechanisms of I_{AB} channels, slowing down their opening. This conclusion is in agreement with the shift in the voltage-dependence of I_{AB}, because higher hyperpolarizations could partly counteract Cd^{2+} effects.

Blockade of I_L. The blocking effect of Cd^{2+} upon the instantaneous linear current I_L is an intriguing result. The Cd^{2+} blockade of G_L was dose-dependent (but never total, saturating between 3 to 10 mM Cd^{2+}) and highly variable between different fibers. Therefore, a precise quantitative description of the Cd^{2+} blockade of G_L could not be performed. Nevertheless, it was always clear that G_L was not totally reduced at $[Cd^{2+}]_o$ which totally abolished G_{AB} (Fig. 1). Therefore, although the Cd^{2+} sensitive component of I_L could result from the same channel as I_{AB}, the above evidence argues in favor of different entities for I_L and I_{AB} channels which are blocked by low concentrations of extracellular Cd^{2+}. Alternatively, the variability of the Cd^{2+} blockade of I_L and the Cd^{2+} resistance of part of I_L could be explained if I_L is a combination of currents through Cd^{2+}-sensitive I_{AB} channels and Cd^{2+}-insensitive leak channels.

We thank Drs. J. Lerma (Instituto Cajal) and J. López-Barneo (Universidad de Sevilla, Spain) for helpful discussion, and one of the anonymous reviewers for his helpful suggestions, specially on the kinetic model.

This work was supported by DGICYT (Spain) and CEC DGXII/PVD and /HCM (Europe) grants to W. Buño, and by an Hispano-French Integrated Action to Dr. François Clarac and W. Buño. A. Araque is a Fundación Areces postdoctoral fellow.

Original version received 18 May 1994 and accepted version received 1 February 1995.

REFERENCES

Adler, E. M., G. J. Augustine, S. N. Duffy, and M. P. Charlton. 1991. Alien intracellular calcium chelators attenuate neurotransmitter release at the squid giant synapse. *Journal of Neuroscience.* 11:1496–1507.

Araque, A., and W. Buño. 1994. Novel hyperpolarization-activated K^+ current mediates anomalous rectification in crayfish muscle. *Journal of Neuroscience.* 14:399–408.

Armstrong, C. M. 1975. Ionic pores, gates, and gating currents. *Quarterly Review of Biophysics.* 7:179–210.

Armstrong, C. M., and J. López-Barneo. 1987. External calcium ions are required for potassium channel gating in squid neurons. *Science.* 236:712–714.

Catterall, W. A. 1980. Neurotoxins that act on voltage-sensitive sodium channels in excitable membranes. *Annual Review of Pharmacology and Toxicology.* 20:15–43.

Chesnoy-Marchais, D. 1983. Characterization of a chloride conductance activated by hyperpolarization in *Aplysia* neurones. *Journal of Physiology.* 342:277–308.

Edman, A., and W. Grampp. 1989. Ion permeation through hyperpolarization-activated membrane channels (Q-channels) in the lobster stretch receptor neurone. *Pflügers Archiv.* 413:249–255.

Frankenhaeuser, B., and A. L. Hodgkin. 1957. The action of calcium on the electrical properties of squid axons. *Journal of Physiology.* 137:218–244.

Ganfornina, M. D., and J. López-Barneo. 1992. Gating of O_2-sensitive K^+ channels of arterial chemoreceptor cells and kinetic modifications induced by low Po_2. *Journal of General Physiology.* 100:427–455.

Gay, L. A., and P. R. Stanfield. 1977. Cs^+ causes a voltage-dependent block of inward K currents in resting skeletal muscle fibers. *Nature.* 267:169–170.

Gilly, W. F., and C. M. Armstrong. 1982. Slowing of sodium channel opening kinetics in squid axon by extracellular zinc. *Journal of General Physiology.* 79:935–964.

Hagiwara, S., and K. Takahashi. 1974. The anomalous rectification and cation selectivity of the membrane of a starfish egg cell. *Journal of Membrane Biology.* 18:61–80.

Hess, P., J. B. Lansman, and R. W. Tsien. 1986. Calcium channel selectivity for divalent and monovalent cations: voltage and concentration dependence of single channel current in ventricular heart cells. *Journal of General Physiology.* 88:293–319.

Hess, P., and R. W. Tsien. 1984. Mechanism of ion permeation through calcium channels. *Nature.* 309:453–456.

Hille, B. 1992. Ionic Channels of Excitable Membranes. Second edition, Sinaur Associates, Inc., Sunderland, MA.

Katz, B., and S. Thesleff. 1957. A study of the "desensitization" produced by acetylcholine at the motor end-plate. *Journal of Physiology.* 138:63–80.

Lansman, J. B. 1990. Blockade of current through single calcium channels by trivalent lanthanide cations: effect of ionic radius on the rates of ion entry and exit. *Journal of General Physiology.* 95:679–696.

Lansman, J. B., P. Hess, and R. W. Tsien. 1986. Blockade of current through single calcium channels by Cd^{2+}, Mg^{2+}, and Ca^{2+}: voltage and concentration dependence of calcium entry into the pore. *Journal of General Physiology.* 88:321–347.

Lester, H. A. 1991. Strategies for studying permeation at voltage-gated ion channels. *Annual Review of Physiology.* 53:477–496.

Matsuda, H., A. Saigusa, and H. Irisawa. 1987. Ohmic conductance through the inwardly rectifying K^+ channel and blocking by internal Mg^{2+}. *Nature.* 325:156–159.

Mayer, M. L., and G. L. Westbrook. 1983. A voltage-clamp analysis of inward (anomalous) rectification in mouse spinal sensory ganglion neurones. *Journal of Physiology.* 340:19–45.

Mlinar, B., and J. Enyeart. 1993. Block of current through T-type calcium channels by trivalent metal cations and nickel in neural rat and human cells. *Journal of Physiology.* 469:639–652.

Nachsen, D. A. 1984. Selectivity of the Ca binding site in synaptosome Ca channels: inhibition of Ca influx by multivalent metal cations. *Journal of General Physiology.* 83:941–967.

Sakmann, B., and G. Trube. 1984. Conductance properties of single inwardly rectifying potassium channels in ventricular cells from guinea-pig heart. *Journal of Physiology.* 347:641–657.

Standen, N. B., and P. R. Stanfield. 1978. A potential- and time-dependent blockade of inward rectification in frog skeletal muscle fibres by barium and strontium ions. *Journal of Physiology.* 280:169–191.

Swandulla, D., and C. M. Armstrong. 1989. Calcium channel block by cadmium in chicken sensory neurons. *Proceedings of the National Academy of Sciences, USA.* 86:1736–1740.

Van Harreveld, A. 1936. A physiological solution for fresh water crustaceans. *Proceedings of the Society for Experimental Biology and Medicine.* 34:428–432.

Woodhull, A. M. 1973. Ionic blockage of sodium channels in nerve. *Journal of General Physiology.* 61:687–708.